PHYSICAL REVIEW D **85,** 054511 (2012)

Deuteron and exotic two-body bound states from lattice QCD

S. R. Beane,[1] E. Chang,[2] W. Detmold,[3,4] H. W. Lin,[5] T. C. Luu,[6] K. Orginos,[3,4] A. Parreño,[2] M. J. Savage,[5] A. Torok,[7] and A. Walker-Loud[8]

(NPLQCD Collaboration)

[1]*Department of Physics, University of New Hampshire, Durham, New Hampshire 03824-3568, USA*
[2]*Department d'Estructura i Constituents de la Matèria. Institut de Ciències del Cosmos (ICC), Universitat de Barcelona, Martí i Franquès 1, E08028-Spain*
[3]*Department of Physics, College of William and Mary, Williamsburg, Virginia 23187-8795, USA*
[4]*Jefferson Laboratory, 12000 Jefferson Avenue, Newport News, Virginia 23606, USA*
[5]*Department of Physics, University of Washington, Box 351560, Seattle, Washington 98195, USA*
[6]*N Division, Lawrence Livermore National Laboratory, Livermore, California 94551, USA*
[7]*Department of Physics, Indiana University, Bloomington, Indiana 47405, USA*
[8]*Lawrence Berkeley National Laboratory, Berkeley, California 94720, USA*

(Received 15 September 2011; published 29 March 2012)

Results of a high-statistics, multivolume lattice QCD exploration of the deuteron, the dineutron, the H-dibaryon, and the $\Xi^-\Xi^-$ system at a pion mass of $m_\pi \sim 390$ MeV are presented. Calculations were performed with an anisotropic $n_f = 2 + 1$ clover discretization in four lattice volumes of spatial extent $L \sim 2.0$, 2.5, 2.9, and 3.9 fm, with a lattice spacing of $b_s \sim 0.123$ fm in the spatial direction and $b_t \sim b_s/3.5$ in the time direction. Using the results obtained in the largest two volumes, the $\Xi^-\Xi^-$ is found to be bound by $B_{\Xi^-\Xi^-}0 = 14.0(1.4)(6.7)$ MeV, consistent with expectations based upon phenomenological models and low-energy effective field theories constrained by nucleon-nucleon and hyperon-nucleon scattering data at the physical light-quark masses. Further, we find that the deuteron and the dineutron have binding energies of $B_d = 11(05)(12)$ MeV and $B_{nn} = 7.1(5.2)(7.3)$ MeV, respectively. With an increased number of measurements and a refined analysis, the binding energy of the H-dibaryon is $B_H = 13.2(1.8)(4.0)$ MeV at this pion mass, updating our previous result.

DOI: 10.1103/PhysRevD.85.054511 PACS numbers: 12.38.Gc

I. INTRODUCTION

A major objective for nuclear physicists is to establish the technology with which to reliably calculate the properties and interactions of nuclei and to be able to quantify the uncertainties in such calculations. Achieving this objective will have broad impact, from establishing the behavior of matter under extreme conditions such as those that arise in the interior of neutron stars, to refining predictions for the array of isotopes produced in nuclear reactors, and even to answering anthropic questions about the nature of our Universe. While nuclear phenomenology generally describes experimentally measured quantities, its ability to make high precision and accurate predictions for quantities that cannot be accessed experimentally is limited. This situation is on the verge of dramatically improving. The underlying theory of the strong interactions is known to be QCD, and the computational resources now available are beginning to allow for *ab initio* calculations of basic quantities in nuclear physics. With further increases in computational power and advances in algorithms, this trend will continue and our understanding of, and our ability to calculate, light and exotic nuclei will be placed on a solid foundation.

In nature, two nucleons in the ${}^3S_1 - {}^3D_1$ coupled channels bind to form the simplest nucleus, the deuteron ($J^\pi = 1^+$), with a binding energy of $B_d = 2.224\,644(34)$ MeV, and nearly bind into a dineutron in the ${}^1S_0$ channel. However, little is known experimentally about possible bound states in more exotic channels, for instance, those containing strange quarks. The most famous exotic channel that has been postulated to support a bound state (the H-dibaryon [1]) has the quantum numbers of $\Lambda\Lambda$ (total angular momentum $J^\pi = 0^+$, isospin $I = 0$, and strangeness $s = -2$). In this channel, all six quarks in naive quark models, like the MIT bag model, can be in the lowest-energy single-particle state. Additionally, more extensive analyses using one-boson-exchange (OBE) models [2] and low-energy effective field theories (EFT) [3,4], both constrained by experimentally measured nucleon-nucleon (NN) and hyperon-nucleon (YN) cross sections and the approximate SU(3) flavor symmetry of the strong interactions, suggest that other exotic channels also support bound states. In the limit of SU(3) flavor symmetry, the ${}^1S_0$ channels are in symmetric irreducible representations of $\mathbf{8} \otimes \mathbf{8} = \mathbf{27} \oplus \mathbf{10} \oplus \overline{\mathbf{10}} \oplus \mathbf{8} \oplus \mathbf{8} \oplus \mathbf{1}$, and hence the $\Xi^-\Xi^-$, $\Sigma^-\Sigma^-$, and nn (along with $n\Sigma^-$ and $\Sigma^-\Xi^-$) all transform in the **27**. YN and NN scattering data along with the

leading SU(3) breaking effects, arising from the light-meson and baryon masses, suggest that $\Xi^-\Xi^-$ and $\Sigma^-\Sigma^-$ are bound at the physical values of the light-quark masses [2–4].

Recently, the first steps have been taken towards calculating the binding energies of light nuclei directly from QCD. Early exploratory quenched calculations of the NN scattering lengths [5,6] performed more than a decade ago have been superseded by $n_f = 2 + 1$ calculations within the last few years [7,8] (and added to by further quenched calculations [9,10][1]). Further, the first quenched calculations of the deuteron [12], ^{3}He, and ^{4}He [13] have been performed, along with $n_f = 2 + 1$ calculations of ^{3}He [14] and multibaryon systems containing strange quarks [14]. Efforts to explore nuclei and nuclear matter using the strong coupling limit of QCD have led to some interesting observations [15]. Recently, $n_f = 2 + 1$ calculations by us (NPLQCD) [16], and subsequent $n_f = 3$ calculations by the HALQCD Collaboration [17,18], have provided evidence that the H-dibaryon (with the quantum numbers of $\Lambda\Lambda$) is bound at a pion mass of $m_\pi \sim 390$ MeV at the physical value of the strange quark mass (NPLQCD), and over a range of SU(3) degenerate light-quark masses with $m_\pi \sim 469$–1171 MeV (HALQCD).[2] Extrapolations to the physical light-quark masses suggest that a weakly bound H-dibaryon or a near threshold resonance exists in this channel [19,20].

In this work, which is a continuation of our high-statistics lattice QCD (LQCD) explorations [8,14,21,22], we present evidence for $\Xi^-\Xi^-(^1S_0)$ and H-dibaryon (refining our results presented in Ref. [16]) bound states, and weak evidence, at the $\sim 1\sigma$ level, for a bound deuteron and dineutron at a pion mass of $m_\pi \sim 390$ MeV. The results were obtained from four ensembles of $n_f = 2 + 1$ anisotropic clover gauge-field configurations with a spatial lattice spacing of $b_s \sim 0.123$ fm, an anisotropy of $\xi \sim 3.5$, and with cubic volumes of spatial extent $L \sim 2.0$, 2.5, 2.9, and 3.9 fm.

In Sec. II, a concise description of the specific LQCD technology and computational details relevant to the present two-body bound-state calculations are given. Section III presents the results of the LQCD calculations of the single-baryon masses and dispersion relations (critical for understanding bound systems), and in Sec. IV the results for the bound states are presented. Discussions and our conclusions can be found in Sec. V.

[1]The HALQCD Collaboration has produced energy-dependent, local, and sink-operator-dependent quantities from lattice spatial correlation functions (see, e.g., Refs. [10,11]) that contain the same, but no more, information than the NN energy eigenvalues in the lattice volume(s) and the associated phase shifts via Lüscher's eigenvalue equation.

[2]One should note that both calculations were performed at approximately the same spatial lattice spacing of $b \sim 0.12$ fm.

II. LATTICE QCD CALCULATIONS

Lattice QCD is a technique in which space-time is discretized into a four-dimensional grid and the QCD path integral over the quark and gluon fields at each point in the grid is performed in Euclidean space-time using Monte Carlo methods. A LQCD calculation of a given quantity will differ from its actual value because of the finite volume of the space-time (with $L^3 \times T$ lattice points) over which the fields exist, and the finite separation between space-time points (the lattice spacing). However, such deviations can be systematically removed by performing calculations in multiple volumes with multiple lattice spacings, and extrapolating using the theoretically known functional dependences on each. In the following subsections, we review the details of LQCD calculations relevant to the current work and introduce the ensembles studied herein.

A. Lüscher's method for two-body systems including bound states

The hadron-hadron scattering amplitude below the inelastic threshold can be determined from two-hadron energy levels in the lattice volume using Lüscher's method [23–25]. In the situation where only a single scattering channel is kinematically allowed, the deviation of the energy eigenvalues of the two-hadron system in the lattice volume from the sum of the single-hadron energies is related to the scattering phase shift, $\delta(k)$, at the measured two-hadron energies. For energy eigenvalues above kinematic thresholds where multiple channels contribute, a coupled-channels analysis is required as a single phase shift does not parametrize the S matrix. Such analyses can be performed, but they are not required in the current context. The energy shift for two particles A and B, $\Delta E = E_{AB} - E_A - E_B$, can be determined from the correlation functions for systems containing one and two hadrons. For baryon-baryon systems, correlation functions of the form

$$\begin{aligned} C_{\mathcal{B};\Gamma}(\mathbf{p},t) &= \sum_{\mathbf{x}} e^{i\mathbf{p}\cdot\mathbf{x}}\Gamma^{\beta}_{\alpha}\langle \mathcal{B}_\alpha(\mathbf{x},t)\bar{\mathcal{B}}_\beta(\mathbf{x}_0,0)\rangle C_{\mathcal{B}_1,\mathcal{B}_2;\Gamma}(\mathbf{p}_1,\mathbf{p}_2,t) \\ &= \sum_{\mathbf{x}_1,\mathbf{x}_2} e^{i\mathbf{p}_1\cdot\mathbf{x}_1} e^{i\mathbf{p}_2\cdot\mathbf{x}_2}\Gamma^{\alpha_1\alpha_2}_{\beta_1\beta_2}\langle \mathcal{B}_{1,\alpha_1}(\mathbf{x}_1,t) \\ &\quad \times \mathcal{B}_{2,\alpha_2}(\mathbf{x}_2,t)\bar{\mathcal{B}}_{1,\beta_1}(\mathbf{x}_0,0)\bar{\mathcal{B}}_{2,\beta_2}(\mathbf{x}_0,0)\rangle \end{aligned} \tag{1}$$

are used, where $\mathcal{B}$ denotes a baryon interpolating operator, α_i and β_i are Dirac indices, and the Γ are Dirac matrices that typically project onto particular parity and angular momentum states. The $\langle \ldots \rangle$ denote averaging over the gauge-field configurations and $\mathbf{x}_0$ is the location of the source. The interpolating operators are only constrained by the quantum numbers of the system of interest (angular momentum, baryon number, isospin, strangeness), and the forms are

$$\begin{aligned} p_\alpha(\mathbf{x},t) &= \epsilon^{ijk} u^i_\alpha(\mathbf{x},t)[u^{j\mathsf{T}}(\mathbf{x},t) C\gamma_5 d^k(\mathbf{x},t)], \\ \Lambda_\alpha(\mathbf{x},t) &= \epsilon^{ijk} s^i_\alpha(\mathbf{x},t)[u^{j\mathsf{T}}(\mathbf{x},t) C\gamma_5 d^k(\mathbf{x},t)], \\ \Sigma^+_\alpha(\mathbf{x},t) &= \epsilon^{ijk} u^i_\alpha(\mathbf{x},t)[u^{j\mathsf{T}}(\mathbf{x},t) C\gamma_5 s^k(\mathbf{x},t)], \\ \Xi^0_\alpha(\mathbf{x},t) &= \epsilon^{ijk} s^i_\alpha(\mathbf{x},t)[u^{j\mathsf{T}}(\mathbf{x},t) C\gamma_5 s^k(\mathbf{x},t)], \end{aligned} \tag{2}$$

where C is the charge-conjugation matrix and ijk are color indices. Other hadrons in the lowest-lying octet can be obtained from the appropriate combinations of quark flavors. The brackets in the interpolating operators indicate contraction of spin indices into a spin-0 "diquark." Away from the time slice of the source (in this case $t = 0$), these correlation functions behave as

$$C^{(i,f)}_{\mathcal{H}_A}(\mathbf{p},t) = \sum_n Z^{(i)}_{n;A}(\mathbf{p}) Z^{(f)}_{n;A}(\mathbf{p}) e^{-E^{(A)}_n(\mathbf{p})t}, \tag{3}$$

$$C^{(i,f)}_{\mathcal{H}_A\mathcal{H}_B}(\mathbf{p},-\mathbf{p},t) = \sum_n Z^{(i)}_{n;AB}(\mathbf{p}) Z^{(f)}_{n;AB}(\mathbf{p}) e^{-E^{(AB)}_n(\mathbf{0})t}, \tag{4}$$

where $E^{(A)}_0(\mathbf{0}) = m_A$ and $E^{(AB)}_n(\mathbf{0})$ are the energy eigenvalues of the two-hadron system at rest in the lattice volume. The quantities $Z^{(i)}_{n;X}$ ($Z^{(f)}_{n;X}$) are determined by the overlap of the source (sink) onto the nth energy eigenstate with the quantum numbers of X. At large times, the ratio

$$\frac{C^{(i,f)}_{\mathcal{H}_A\mathcal{H}_B}(\mathbf{p},-\mathbf{p},t)}{C^{(i,f)}_{\mathcal{H}_A}(\mathbf{0},t) C^{(i,f)}_{\mathcal{H}_B}(\mathbf{0},t)} \xrightarrow{t\to\infty} \tilde{Z}^{(i)}_{0,AB}(\mathbf{p}) \tilde{Z}^{(f)}_{0,AB}(\mathbf{p}) e^{-\Delta E^{(AB)}_0(\mathbf{0})t} \tag{5}$$

decays as a single exponential in time with the energy shift $\Delta E^{(AB)}_0(\mathbf{0})$. The $\tilde{Z}^{(k)}_{0,AB}(\mathbf{p})$ are combinations of the two-body and one-body Z factors in Eq. (3). In what follows, only the case $\mathbf{p} = \mathbf{0}$ is considered. The energy shift of the nth two-hadron state,

$$\begin{aligned} \Delta E^{(AB)}_n &\equiv E^{(AB)}_n(\mathbf{0}) - m_A - m_B \\ &= \sqrt{k_n^2 + m_A^2} + \sqrt{k_n^2 + m_B^2} - m_A - m_B, \end{aligned} \tag{6}$$

determines a squared momentum k_n^2 (which can be either positive or negative). Below inelastic thresholds, this is related to the real part of the inverse scattering amplitude via[3]

$$k_n \cot\delta(k_n) = \frac{1}{\pi L} S\left(k_n^2 \left(\frac{L}{2\pi}\right)^2\right), \tag{7}$$

where

$$S(x) = \lim_{\Lambda\to\infty} \sum_{\mathbf{j}}^{|\mathbf{j}|<\Lambda} \frac{1}{|\mathbf{j}|^2 - x} - 4\pi\Lambda, \tag{8}$$

thereby implicitly determining the value of the phase shift at the energy $\Delta E^{(AB)}_n$ [or the momentum of each particle in the center of momentum frame, k_n], $\delta(k_n)$ [23–27]. Thus, the function $k\cot\delta$ that determines the low-energy elastic-scattering cross section, $\mathcal{A}(k) \propto (k\cot\delta(k) - ik)^{-1}$, is determined at the energy $\Delta E^{(AB)}_n$.

In a channel for which one pion exchange is allowed by spin and isospin considerations, the function $k\cot\delta(k)$ is an analytic function of $|\mathbf{k}|^2$ for $|\mathbf{k}| \le m_\pi/2$, as determined by the t-channel cut in the scattering amplitude. In this kinematic regime, $k\cot\delta(k)$ can be expressed in terms of an effective range expansion of the form

$$k\cot\delta(k) = -\frac{1}{a} + \frac{1}{2} r_0 |\mathbf{k}|^2 + \ldots, \tag{9}$$

where a is the scattering length (with the nuclear physics sign convention) and r_0 is the effective range. While the magnitude of the effective range (and higher terms) is set by the pion mass, the scattering length is unconstrained. For scattering processes where one pion exchange does not contribute, the radius of convergence of the effective range expansion of $k\cot\delta$ is set by the lightest intermediate state in the t channel (or by the inelastic threshold).

In the situation where a channel supports a bound state, the energy of the bound state at rest is determined by Eq. (7). For $k_{-1}^2 < 0$, and setting $k_{-1} = i\kappa$, Eq. (7) becomes

$$k\cot\delta(k)|_{k=i\kappa} + \kappa = \frac{1}{L} \sum_{\mathbf{m}\neq\mathbf{0}} \frac{1}{|\mathbf{m}|} e^{-|\mathbf{m}|\kappa L} = \frac{1}{L} F^{(\mathbf{0})}(\kappa L), \tag{10}$$

where

$$F^{(\mathbf{0})}(\kappa L) = 6e^{-\kappa L} + 6\sqrt{2} e^{-\sqrt{2}\kappa L} + \frac{8}{\sqrt{3}} e^{-\sqrt{3}\kappa L} + \ldots. \tag{11}$$

Perturbation theory can be used to solve Eq. (10) when the extent of the volume is much larger than the size of the bound system, giving [26,27]

$$\kappa = \kappa_0 + \frac{Z_\psi^2}{L} F^{(\mathbf{0})}(\kappa_0 L) + \mathcal{O}(e^{-2\kappa_0 L}/L) \quad \text{with} \quad Z_\psi = \frac{1}{\sqrt{1 - 2\kappa_0 \frac{d}{dk^2} k\cot\delta|_{i\kappa_0}}}. \tag{12}$$

κ_0 is the solution to

[3] Calculations performed on anisotropic lattices require a modified energy-momentum relation, and, as a result, Eq. (6) becomes

$$\begin{aligned} \Delta E^{(AB)}_n &\equiv E^{(AB)}_n - m_A - m_B \\ &= \sqrt{k_n^2/\xi_A^2 + m_A^2} + \sqrt{k_n^2/\xi_B^2 + m_B^2} - m_A - m_B, \end{aligned}$$

where $\xi_{A,B}$ are the anisotropy factors for particle A and particle B, respectively, determined from the appropriate energy-momentum dispersion relation. The masses and energy splitting are given in terms of temporal lattice units and k_n is given in spatial lattice units.

TABLE I. Results from the lattice QCD calculations in four lattice volumes with a pion mass of $m_\pi \sim 390$ MeV, a spatial lattice spacing of $b_s \sim 0.123$ fm, and with an anisotropy factor of $\xi \sim 3.5$. Infinite-volume extrapolations [22] are shown in the right column. The masses are in temporal lattice units (t.l.u).

$L^3 \times T$	$16^3 \times 128$	$20^3 \times 128$	$24^3 \times 128$	$32^3 \times 256$	Extrapolation
L (fm)	$\sim$2.0	$\sim$2.5	$\sim$2.9	$\sim$3.9	∞
$m_\pi L$	3.86	4.82	5.79	7.71	∞
$m_\pi T$	8.82	8.82	8.82	17.64	∞
M_N (t.l.u.)	0.210 04(44)(85)	0.206 82(34)(45)	0.204 63(27)(36)	0.204 57(25)(38)	0.204 55(19)(17)
M_Λ (t.l.u.)	0.224 46(45)(78)	0.222 46(27)(38)	0.220 74(20)(42)	0.220 54(23)(31)	0.220 64(15)(19)
M_Σ (t.l.u.)	0.228 61(38)(67)	0.227 52(32)(43)	0.227 91(24)(31)	0.227 26(24)(43)	0.227 47(17)(19)
M_Ξ (t.l.u.)	0.241 92(38)(63)	0.241 01(27)(38)	0.239 75(20)(32)	0.239 74(17)(31)	0.239 78(12)(18)

$$k \cot\delta(k)|_{k=i\kappa_0} + \kappa_0 = 0, \tag{13}$$

which recovers $\cot\delta(k)|_{k=i\kappa_0} = +i$, and is the infinite-volume binding momentum of the system. This analysis has recently been extended to bound systems that are moving in the lattice volume [28,29].

B. Computational overview

Anisotropic gauge-field configurations have proven useful for the study of hadronic spectroscopy, and as the calculations required for studying multihadron systems rely heavily on spectroscopy, considerable effort has been put into calculations with clover-improved Wilson fermion actions with an anisotropic discretization. In particular, the $n_f = 2 + 1$ flavor anisotropic clover Wilson action [30,31], with two steps of stout-link smearing [32] of the spatial gauge fields in the fermion action with a smearing weight of $\rho = 0.14$, has been used [33,34]. The gauge fields entering the fermion action are not smeared in the time direction, thus preserving the ultralocality of the action in the time direction. Further, a tree-level tadpole-improved Symanzik gauge action without a 1×2 rectangle in the time direction is used. Anisotropy allows for a better extraction of the excited states as well as additional confidence that plateaus in the effective mass plots (EMPs) formed from the correlation functions have been observed, significantly reducing the systematic uncertainties. The gauge-field generation was performed by the Hadron Spectrum Collaboration (HSC) and by us, and these gauge-field configurations have been extensively used for excited hadron spectrum calculations by HSC [35–40].

The present calculations are performed on four ensembles of gauge configurations with $L^3 \times T$ of $16^3 \times 128$, $20^3 \times 128$, $24^3 \times 128$, and $32^3 \times 256$ lattice sites, with an anisotropy of $b_t = b_s/\xi$ with $\xi \sim 3.5$. The spatial lattice spacing of each ensemble is $b_s \sim 0.1227 \pm 0.008$ fm, giving spatial lattice extents of $L \sim 2.0$, 2.5, 2.9, and 3.9 fm, respectively. The same input light-quark-mass parameters, $b_t m_l = -0.0840$ and $b_t m_s = -0.0743$, are used in the production of each ensemble, giving a pion mass of $m_\pi \sim 390$ MeV. The relevant quantities to assign to each ensemble that determine the impact of the finite lattice volume are $m_\pi L$ and $m_\pi T$, which, for the four ensembles, are $m_\pi L \sim 3.86$, 4.82, 5.79, and 7.71, respectively, and $m_\pi T \sim 8.82$, 8.82, 8.82, and 17.64.

For the four lattice ensembles, multiple light-quark propagators were calculated on each configuration. The source location was chosen randomly in order to minimize correlations among propagators. On the $\{16^3 \times 128, 20^3 \times 128, 24^3 \times 128, 32^3 \times 256\}$ ensembles, an average of $\{224, 364, 178, 174\}$ propagators were calculated on each of $\{2001, 1195, 2215, 739\}$ gauge-field configurations, to give a total number of $\sim\{4.5, 4.3, 3.9, 1.3\} \times 10^5$ light-quark propagators, respectively.[4]

III. BARYONS AND THEIR DISPERSION RELATIONS

The single-hadron masses calculated in the four different lattice volumes are given in Table I. Detailed discussions of the fitting methods used in the analysis of the correlation functions are given in Refs. [8,14,21,41]. Infinite-volume extrapolations of the results obtained from all four ensembles were performed in Ref. [22], and are shown in the right-most column in Table I. The difference between a mass calculated in a finite lattice volume and its infinite-volume extrapolation is due to contributions of the form $\sim e^{-m_\pi L}$. Such deviations must be small compared to the two-body binding energies to ensure that the finite-volume bindings are due to the T matrix [42,43] and not from finite-volume distortions of the forces. It has been shown [16,22] that the largest two volumes, the $24^3 \times 128$ and $32^3 \times 256$ ensembles, are sufficiently large to render the $\sim e^{-m_\pi L}$ modifications to Lüscher's eigenvalue relation negligible at the level of precision we are currently able to achieve. In what follows, we only consider results from these ensembles.

Lüscher's method assumes that the single-hadron energy-momentum relation is satisfied over the range of energies used in Eq. (7). In order to verify that the energy-momentum relation is satisfied, single-hadron correlation

[4]One propagator is defined to include the four spin and three color degrees of freedom; i.e. it is the propagator for all 12 spin-color components.

TABLE II. The anisotropy parameter ξ_H of each hadron from the $32^3 \times 256$ ensemble using the continuum dispersion relation in Eq. (14) and the lattice dispersion relation in Eq. (15). The result for the π is included for purposes of comparison.

	N	Λ	Σ	Ξ	π
ξ_H (continuum)	3.559(27)(08)	3.465(31)(06)	3.456(35)(07)	3.4654(55)(14)	3.466(13)(02)
ξ_H (lattice)	3.487(34)(10)	3.399(63)(16)	3.387(72)(15)	3.396(40)(07)	3.435(25)(10)

functions were formed with well-defined lattice spatial momentum $\mathbf{p} = \frac{2\pi}{L}\mathbf{n}$ for $|\mathbf{n}|^2 \leq 5$. Retaining the leading terms in the energy-momentum relation, including the lattice anisotropy ξ, the energy and mass of the hadron [in temporal lattice units (t.l.u)], and the momentum in spatial lattice units (s.l.u.) are related by

$$(b_t E_H(|\mathbf{n}|^2))^2 = (b_t M_H)^2 + \frac{1}{\xi^2}\left(\frac{2\pi b_s}{L}\right)^2 |\mathbf{n}|^2, \qquad (14)$$

using the continuum dispersion relation, and by

$$(b_t E_H(|\mathbf{n}|^2))^2 = (b_t M_H)^2 + \frac{1}{\xi^2}\sum_j \sin^2\left(\frac{2\pi b_s}{L} n_j\right), \qquad (15)$$

using the lattice dispersion relation. The calculated single-hadron energies (squared) are shown in Fig. 1 as a function of $|\mathbf{n}|^2$, along with the best linear fit. The extracted values of ξ_H are given in Table II, and are seen to be consistent with each other within the uncertainties of the calculation (the value for the nucleon is somewhat larger). Notice that the lattice dispersion relation gives rise to ξ_H that is slightly smaller than those from the continuum dispersion relation, and with somewhat larger uncertainties. The values of ξ_H from the continuum dispersion relation are used to convert the two-hadron energies and energy differences from temporal lattice units into spatial lattice units which are then used in the Lüscher eigenvalue relation. In physical units, using the continuum values of ξ_H given in Table II, the extrapolated baryon masses are $M_N = 1170.0(1.1)(1.0)(7.5)(9.3)$ MeV, $M_\Lambda = 1229.5(0.8)(1.1)(8.1)(11.2)$ MeV, $M_\Sigma = 1264.2(1.0) \times (1.1)(8.3)(13.1)$ MeV, and $M_\Xi = 1336.3(0.7)(1.0)(8.8) \times (21.9)$ MeV, where the first uncertainty is statistical, the second is systematic, the third is from the lattice spacing, and the fourth is from ξ_H.

IV. TWO-BODY BOUND STATES

Of the baryon-baryon channels that we have explored at this pion mass, the states that have an energy lower than two isolated baryons in both the $24^3 \times 128$ and $32^3 \times 256$ ensembles and suggest the existence of bound states are the

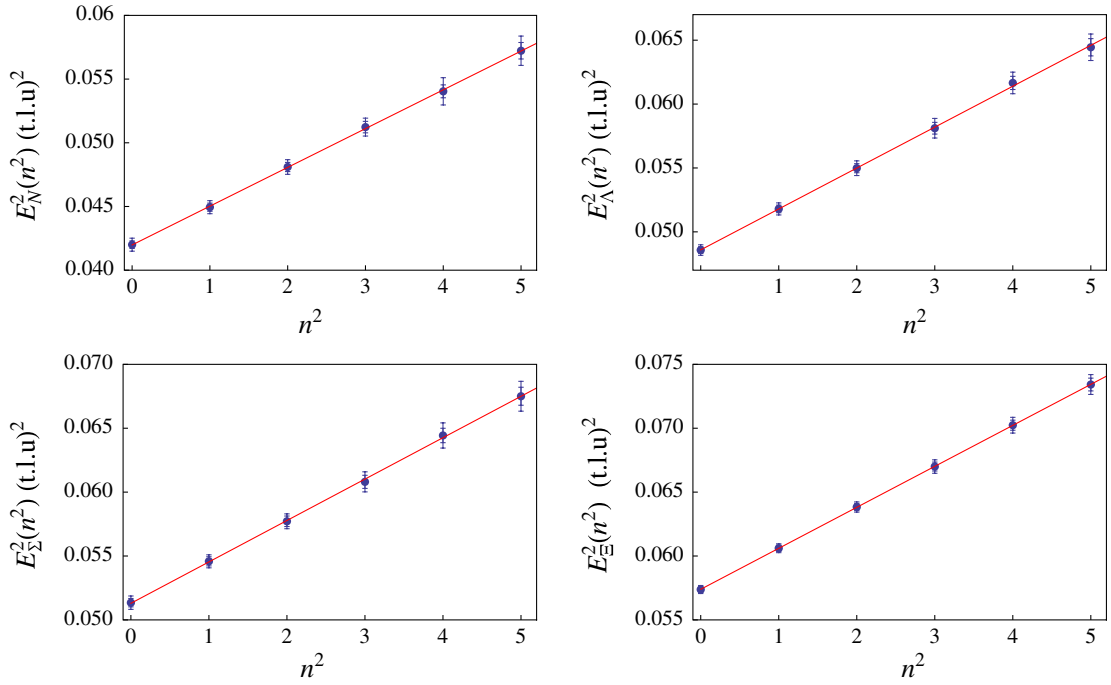

FIG. 1 (color online). The squared energy [in (t.l.u.)^2] of the single-baryon states as a function of $n^2 = |\mathbf{n}|^2$, related to the squared momentum, $|\mathbf{p}|^2 = (\frac{2\pi}{L})^2|\mathbf{n}|^2$, calculated with the $32^3 \times 256$ ensemble. The blue points are the results of the LQCD calculations with the inner (outer) uncertainties being the statistical uncertainties (statistical and systematic uncertainties combined in quadrature). The red curves correspond to the best linear fits.

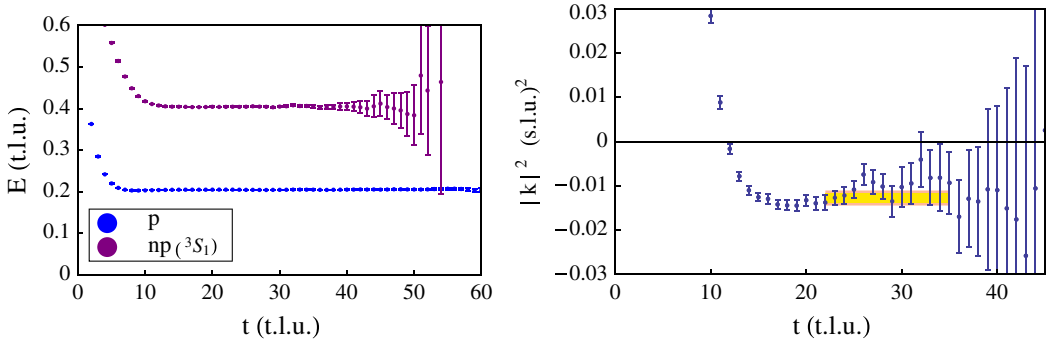

FIG. 2 (color online). The left panel shows an EMP of the nucleon and of the neutron-proton system in the $^3S_1 - {}^3D_1$ coupled-channels calculated with the $24^3 \times 128$ ensemble (in t.l.u.). The right panel shows the $|\mathbf{k}|^2$ (in (s.l.u.)^2) of the neutron-proton system calculated with this ensemble, along with the fits.

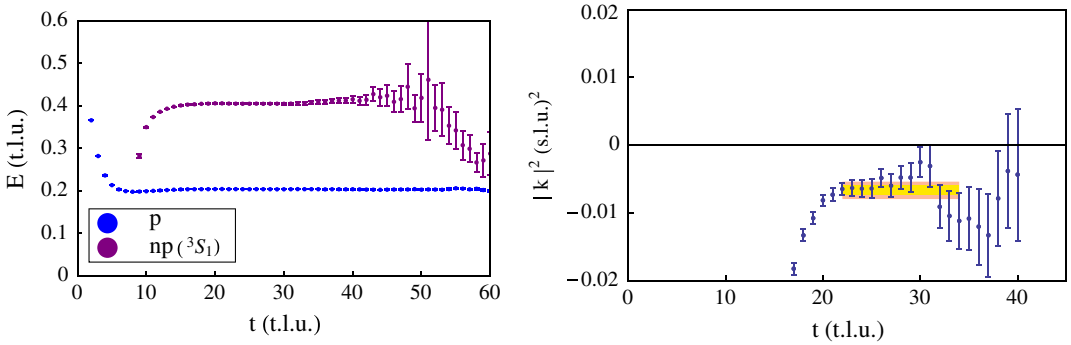

FIG. 3 (color online). The left panel shows an EMP of the nucleon and of the neutron-proton system in the $^3S_1 - {}^3D_1$ coupled channels calculated with the $32^3 \times 256$ ensemble (in t.l.u.). The right panel shows the $|\mathbf{k}|^2$ [in (s.l.u.)^2] of the neutron-proton system calculated with this ensemble, along with the fits.

deuteron, the dineutron, the H-dibaryon, and the $\Xi^-\Xi^-$. While a negative energy shift can indicate either a scattering state with an attractive interaction or a bound state, Lüscher's eigenvalue relation allows us to distinguish between the two possibilities. For a bound system in the large-volume limit, the calculated value of the energy splitting (or binding momentum) gives rise to $-i\cot\delta \longrightarrow +1$. We now examine each of these channels.

A. The deuteron

The deuteron is the simplest nucleus, comprised of a neutron and a proton. At the physical light-quark masses its binding energy is $B = 2.224\,644(34)$ MeV which corresponds to a binding momentum of $\kappa_0 \sim 45.70$ MeV (using the isospin averaged nucleon mass of $M_N = 938.92$ MeV). As it is a spin-1 system composed of two spin-$\frac{1}{2}$ nucleons, its wave function is an admixture of s waves and d waves, but at the physical quark masses it is known to be predominantly s wave with only a small admixture of d wave induced by the tensor ($L = S = 2$) interaction.

The EMPs associated with the nucleon and the neutron-proton system in the $^3S_1 - {}^3D_1$ channel are shown in the left panels of Figs. 2 and 3 for the two ensembles. The correlation functions that give rise to these EMPs are linear combinations of correlation functions generated using Eq. (1) but with different smearings of the sink operator (s). The combinations of correlation functions have been chosen to maximize the extent of the ground-state plateaus.[5] Extended plateaus are observed in both the one- and two-nucleon correlation functions. The right panels of Figs. 2 and 3 show the binding momentum of each particle in the center of momentum frame obtained by taking ratios of the two-baryon and single-baryon correlation functions. The deuteron binding energies in each volume calculated with LQCD are

[5]The EMPs result from a matrix-Prony analysis [21] of multiple correlation functions. In particular, the matrix-Prony analysis is used to determine the linear combination of correlation functions that optimizes the ground-state plateau. The EMPs that are shown for each system result from these linear combinations and not from the energy eigenvalues resulting from the matrix-Prony analysis. In determining the binding energies, multiexponential fitting and generalized pencil of function methods [44,45] are used in addition to matrix-Prony, which provides consistent results in each case.

$$B_d^{(L=24)} = 22.3 \pm 2.3 \pm 5.4 \text{ MeV},$$
$$B_d^{(L=32)} = 14.9 \pm 2.3 \pm 5.8 \text{ MeV}. \quad (16)$$

The known finite-volume dependence of loosely bound systems, given in Eq. (10), and the perturbative relations that follow allow for an extrapolation of the results in Eq. (16) to the infinite-volume limit, as shown in Fig. 4, giving

$$B_d^{(L=\infty)} = 11 \pm 5 \pm 12 \text{ MeV}, \quad (17)$$

where the first uncertainty is statistical and the second is systematic, accounting for fitting, anisotropy, lattice spacing, and the infinite-volume extrapolation. Despite having statistically significant binding energies in the two lattice volumes, the exponential extrapolation to the infinite-volume limit produces a deuteron binding energy with significance at $\sim 1\sigma$. From the curvature of the results of the LQCD calculations in Fig. 4, it is clear that both of these volumes significantly modify the deuteron at this pion mass. Calculations in somewhat larger volumes, or of moving systems [29], would significantly reduce the uncertainty introduced by the volume extrapolation.

It is interesting to note that while the ground-state energies obtained in both the $24^3 \times 128$ and $32^3 \times 256$ ensembles are clearly negatively shifted in energy and lie on the bound-state branch of the S function ($k^2 < 0$ with $k \cot\delta < 0$) in Eq. (8), the result from the $20^3 \times 128$ ensemble is consistent with both a bound state and a continuum state. It is important for future LQCD calculations in this channel to precisely determine the volume dependence of the ground-state energies in order to better quantify the exponential corrections to Lüscher's energy-eigenvalue relation.

Our $n_f = 2 + 1$ result and the recent quenched ($n_f = 0$) result of Ref. [12] are shown in Fig. 5, along with the physical deuteron binding energy. Clearly, the large uncertainty of our present result does not provide much constraint on the dependence of the deuteron binding energy as a function of the light-quark masses, other than to demonstrate that the deuteron is likely bound at $m_\pi \sim 390$ MeV, qualitatively consistent with the quenched result at $m_\pi \sim 800$ MeV [12].

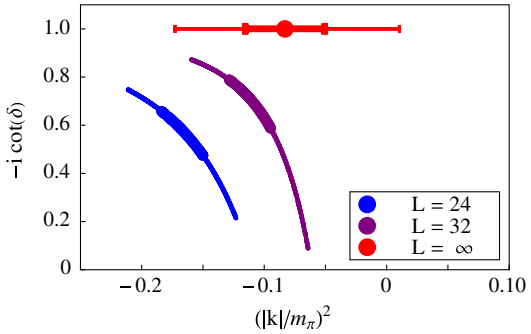

FIG. 4 (color online). Results of the lattice QCD calculations of $-i\cot\delta$ versus $|\mathbf{k}|^2/m_\pi^2$ in the deuteron channel obtained using Eq. (7), along with the infinite-volume extrapolation using Eq. (10). The inner uncertainty associated with each point is statistical, while the outer corresponds to the statistical and systematic uncertainties combined in quadrature.

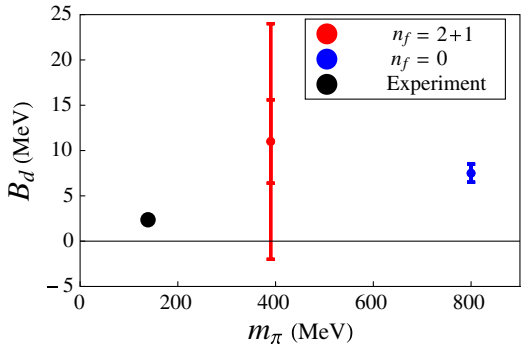

FIG. 5 (color online). The deuteron binding energy as a function of the pion mass. The black circle denotes the experimental value. The blue point and uncertainty result from the quenched calculations of Ref. [12], while the red point and uncertainty (the inner is statistical and the outer is statistical and systematic combined in quadrature) show our present $n_f = 2 + 1$ result.

A number of groups have attempted to determine how the deuteron binding energy (and the binding of other nuclei) varies as a function of the light-quark masses using EFT [46–49] and hadronic models [50]. Such a variation impacts the constraints that can be placed on possible time variations of the fundamental constants of nature from the abundance of elements produced in big bang nucleosynthesis (BBN) (see Refs. [51,52] for recent constraints from BBN). With the exception of the analysis of Ref. [49], both of the EFT analyses, which use naive dimensional analysis to constrain the quark-mass-dependent dimension-six operators that contribute at next-to-leading order in the chiral expansion, and the hadronic models of Ref. [50], suggest that the deuteron becomes less bound as the quarks become heavier near their physical values. The present LQCD calculation at a pion mass of $m_\pi \sim 390$ MeV is somewhat beyond the range of applicability of the EFT analyses and so cannot be directly translated into constraints on the coefficients of local operators with confidence. Further, the uncertainty in our calculation is too large to be useful in a quantitative way. Nevertheless, our result conflicts with the trend suggested in most of the EFT and model analyses, and further studies are necessary to resolve this issue.

B. The dineutron

In nature, the dineutron ($nn\ ^1S_0$) is very nearly bound. The unnaturally large scattering lengths in the $^1S_0$ channel indicate that a very small increase in the strength of the interactions between neutrons would bind them into an electrically neutral nucleus. If the binding was deep enough, it would have profound effects on nucleosynthesis.

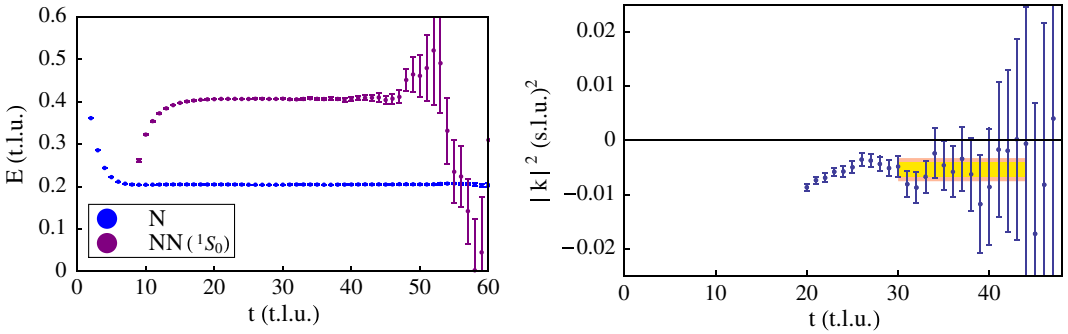

FIG. 6 (color online). The left panel shows an EMP of the neutron and of the neutron-neutron system calculated with the $24^3 \times 128$ ensemble (in t.l.u.). The right panel shows the $|\mathbf{k}|^2$ [in (s.l.u.)^2] of the neutron-neutron system calculated with this ensemble, along with the fits.

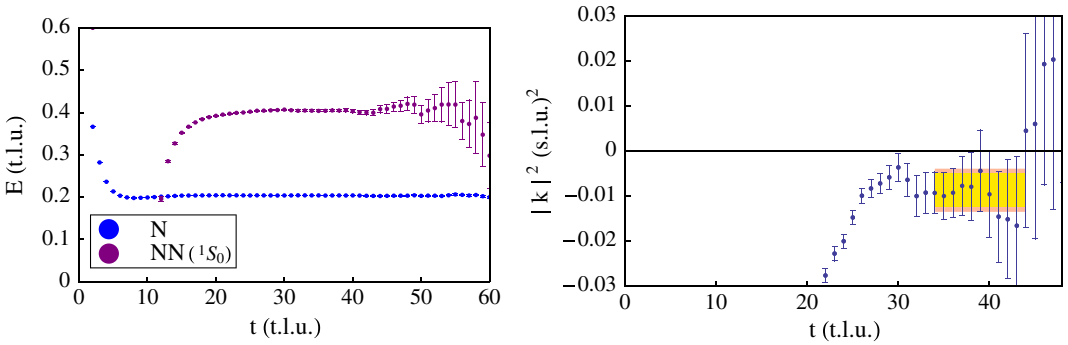

FIG. 7 (color online). The left panel shows an EMP of the neutron and of the neutron-neutron system calculated with the $32^3 \times 256$ ensemble (in t.l.u.). The right panel shows the $|\mathbf{k}|^2$ [in (s.l.u.)^2] of the neutron-neutron system calculated with this ensemble, along with the fits.

Analyses with NNEFT allow for the possibility of both bound and unbound dineutrons for light-quark masses larger than those of nature, while indicating an unbound dineutron for lighter quark masses [46–48]. In contrast, a model-dependent calculation indicates that the dineutron remains unbound for all light-quark masses [50].

The EMPs associated with the nucleon and the dineutron system are shown in the left panels of Figs. 6 and 7. The dineutron binding energies extracted from the LQCD calculations are

$$\begin{aligned} B_{nn}^{(L=24)} &= 10.4 \pm 2.6 \pm 3.1 \text{ MeV}, \\ B_{nn}^{(L=32)} &= 8.3 \pm 2.2 \pm 3.3 \text{ MeV}. \end{aligned} \tag{18}$$

The volume extrapolation of the results in Eq. (18) is shown in Fig. 8, and it results in an extrapolated dineutron binding energy of

$$B_{nn}^{(L=\infty)} = 7.1 \pm 5.2 \pm 7.3 \text{ MeV}, \tag{19}$$

where the first uncertainty is statistical and the second is systematic. This result is suggestive of a bound dineutron at this pion mass, but at the present level of precision, an unbound system is also possible. In the $L \sim 2.5$ fm volume, the dineutron ground state is found to be positively shifted in energy at the 1σ level [8], consistent with both a bound state and a continuum state. Further computational resources devoted to the smaller-volume ensemble would allow for better understanding of the volume dependence of this state and, in general, would be a valuable component of future studies.

Our $n_f = 2 + 1$ result and the recent quenched ($n_f = 0$) result of Ref. [12] are shown in Fig. 9. Clearly, the large uncertainty of our present result does not provide a significant constraint on the binding of the dineutron as a function of the light-quark masses. However, the LQCD results suggest that the dineutron is bound at quark masses greater than those of nature. This has implications for future LQCD calculations, as there are likely light-quark masses for which the dineutron unbinds, and hence the scattering length becomes infinitely large. This implies that, at some point in the future, LQCD may be able to explore strongly interacting systems of fermions near the unitary limit. However, if the deuteron remains bound at heavier quark masses, as suggested by the current work, it may not be possible to tune the light-quark masses (including isospin breaking) to produce infinite scattering lengths in the $^3S_1 - {}^3D_1$ and $^1S_0$ channels simultaneously, hence eliminating the possibility of the triton having an infinite

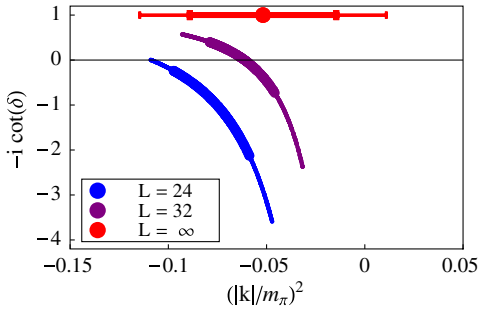

FIG. 8 (color online). The results of the lattice QCD calculations of $-i\cot\delta$ versus $|\mathbf{k}|^2/m_\pi^2$ in the dineutron channel obtained using Eq. (7), along with the infinite-volume extrapolation using Eq. (10). The inner uncertainty associated with each point is statistical, while the outer corresponds to the statistical and systematic uncertainties combined in quadrature.

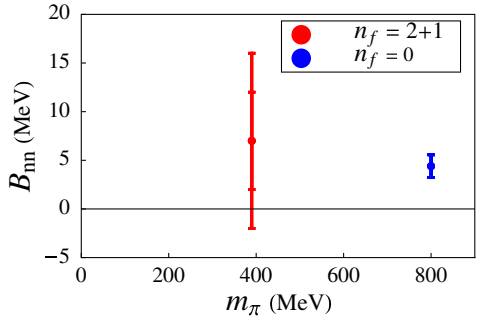

FIG. 9 (color online). The dineutron binding energy as a function of the pion mass. The blue point and uncertainty result from the quenched calculation of Ref. [12], while the red point and uncertainty (the inner is statistical and the outer is statistical and systematic combined in quadrature) show our present $n_f = 2 + 1$ result.

number of bound states for such a specific choice of light-quark masses (unless the deuteron is also unbound for an intermediate range of quark masses).[6]

C. The H-dibaryon

The prediction of a relatively deeply bound system with the quantum numbers of $\Lambda\Lambda$ (called the H-dibaryon) by Jaffe [1] in the late 1970s, based upon a bag-model calculation, started a vigorous search for such a system, both experimentally and also with alternate theoretical tools. As all six quarks, *uuddss*, can be in an *s* wave and satisfy the Pauli principle, such a channel may support a state that is more deeply bound than in channels with different flavor quantum numbers. Reviews of experimental constraints on, and phenomenological models of, the H-dibaryon can be found in Refs. [54–57]. While experimental studies of doubly strange ($s = -2$) hypernuclei restrict the H-dibaryon to be unbound or to have a small binding energy, the most recent constraints on the existence of the H-dibaryon come from heavy-ion collisions at the Relativistic Heavy Ion Collider [58], effectively eliminating the possibility of a loosely bound H-dibaryon at the physical light-quark masses. However, the analysis that led to these constraints was model dependent, in particular, in the production mechanism, and may simply not be reliable. Recent experiments at KEK indicate that a near threshold resonance may exist in this channel [59].

A number of quenched LQCD calculations [60–65] have previously searched for the H-dibaryon, but without success. Recently, we and the HALQCD Collaboration have reported results that show that the H-dibaryon is bound for a range of light-quark masses that are larger than those found in nature [16,17]. At present, neither of these calculations is extrapolated to the continuum, with both calculations being performed at a spatial lattice spacing of $b_s \sim 0.12$ fm. Chiral extrapolations in the light-quark masses of these two LQCD calculations were performed in Refs. [19,20] to make first QCD predictions for the binding energy of the H-dibaryon at the physical light-quark masses.[7]

In the absence of interactions, the $\Lambda\Lambda - \Xi N - \Sigma\Sigma$ coupled system (all three have the same quantum numbers) is expected to exhibit three low-lying eigenstates, as the mass splittings between the single-particle states are (from the $32^3 \times 256$ ensemble)

$$\begin{aligned} 2(M_\Sigma - M_\Lambda) &= 0.013\,17(13)(19)\ \text{t.l.u.}, \\ M_\Xi + M_N - 2M_\Lambda &= 0.003\,397(61)(65)\ \text{t.l.u.} \end{aligned} \tag{20}$$

However, if the interaction generates a bound state, it is unlikely that a second or third state will also be bound, and therefore the splitting between the ground state and the two additional states will likely be larger than estimates based upon the single-baryon masses. The EMPs associated with the Λ and the system with the quantum numbers of the $\Lambda\Lambda$

[6]Such bound states would be the manifestation of an infrared renormalization group limit cycle in QCD, as conjectured by Braaten and Hammer [53].

[7]These extrapolations are significantly less reliable (rigorous) than the chiral extrapolation of simple quantities (such as hadron masses) calculated with LQCD. While for a deeply bound H-dibaryon with a radius that is much smaller than the inverse pion mass it is possible to arrive at a chiral EFT construction with which to calculate the light-quark-mass dependence of H-dibaryon mass in perturbation theory, the same construction would not be valid when the radius becomes comparable to or larger than $1/m_\pi$. A weakly bound state can only be generated nonperturbatively, and consequently, the quark-mass dependence of the binding energy is nontrivial, as is clear from the analyses in the two-nucleon sector; see e.g. Refs. [46–48,66]. As a result, the assumption of compactness of the state made in Ref. [20] is difficult to justify over a significant range of predicted binding energies. Further, the simple polynomial extrapolations in Ref. [19] are meant to provide estimates alone and cannot be used to reliably quantify extrapolation uncertainties.

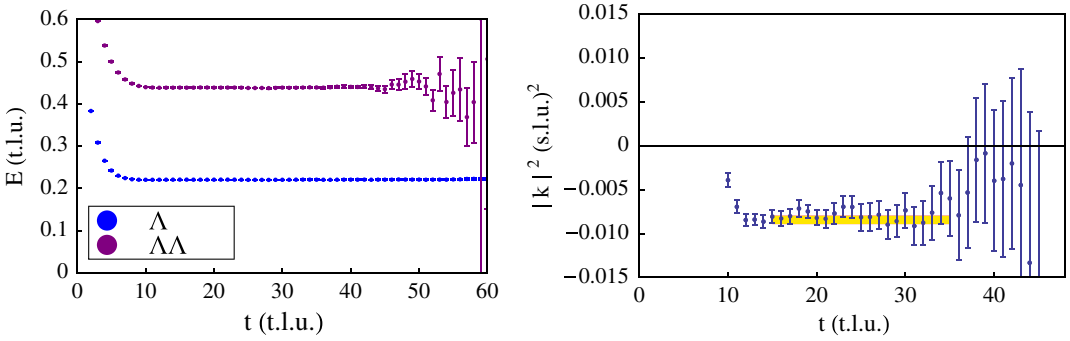

FIG. 10 (color online). The left panel shows an EMP of the Λ and of the lowest state in the $\Lambda\Lambda - \Xi N - \Sigma\Sigma$ system calculated with the $24^3 \times 128$ ensemble (in t.l.u.). The right panel shows the $|\mathbf{k}|^2$ [in (s.l.u.)^2] of the $\Lambda\Lambda - \Xi N - \Sigma\Sigma$ system calculated with this ensemble, along with the fits.

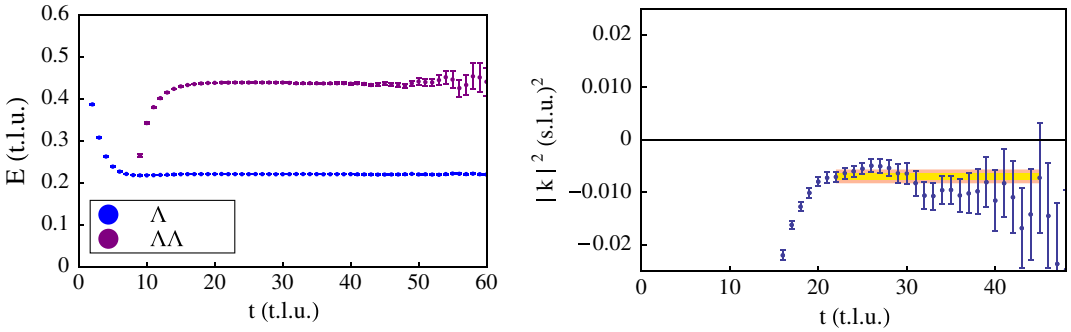

FIG. 11 (color online). The left panel shows an EMP of the Λ and of the lowest state in the $\Lambda\Lambda - \Xi N - \Sigma\Sigma$ system calculated with the $32^3 \times 256$ ensemble (in t.l.u.). The right panel shows the $|\mathbf{k}|^2$ [in (s.l.u.)^2] of the $\Lambda\Lambda - \Xi N - \Sigma\Sigma$ system calculated with this ensemble, along with the fits.

are shown in the left panels of Figs. 10 and 11. The binding energies extracted from the LQCD calculations are

$$B_H^{(L=24)} = 17.52 \pm 0.88 \pm 0.68 \text{ MeV},$$
$$B_H^{(L=32)} = 14.5 \pm 1.3 \pm 2.4 \text{ MeV}, \tag{21}$$

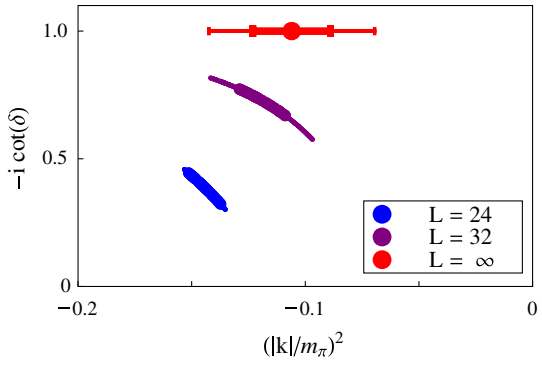

FIG. 12 (color online). The results of the LQCD calculations of $-i\cot\delta$ versus $|\mathbf{k}|^2/m_\pi^2$ in the H-dibaryon channel obtained using Eq. (7), along with the infinite-volume extrapolation using Eq. (10). The inner uncertainty associated with each point is statistical, while the outer corresponds to the statistical and systematic uncertainties combined in quadrature.

which agree within uncertainties with the values given in our earlier paper [16]. The volume extrapolation of the results in Eq. (21) is shown in Fig. 12, and gives an extrapolated H-dibaryon binding energy of

$$B_H^{(L=\infty)} = 13.2 \pm 1.8 \pm 4.0 \text{ MeV}, \tag{22}$$

where the first uncertainty is statistical and the second is systematic. In Ref. [16], $B_H^{(L=\infty)}$ was assigned a volume extrapolation uncertainty of ± 1 MeV. In the present analysis, this systematic uncertainty has been reduced to ± 0.3 MeV by keeping the first three terms in the volume expansion [29] given in Eq. (11) [only the first term in Eq. (11) was used in the extrapolation performed in Ref. [16]]. The uncertainty in the energy-momentum relation is unchanged and is estimated to be ± 0.6 MeV. The updated result in Eq. (22) at $m_\pi \sim 390$ MeV and the result of the $n_f = 3$ calculation at $m_\pi \sim 837$ MeV [17][8] are

[8]In extrapolating to the physical values of the light-quark masses, and in the absence of an extrapolation form that describes the full three-flavor dependence, we use the result from the HALQCD Collaboration with a strange quark mass that is closest to its physical value, and perform an extrapolation in the up- and down-quark masses in the isospin limit. For further discussion of this selection, see Ref. [19].

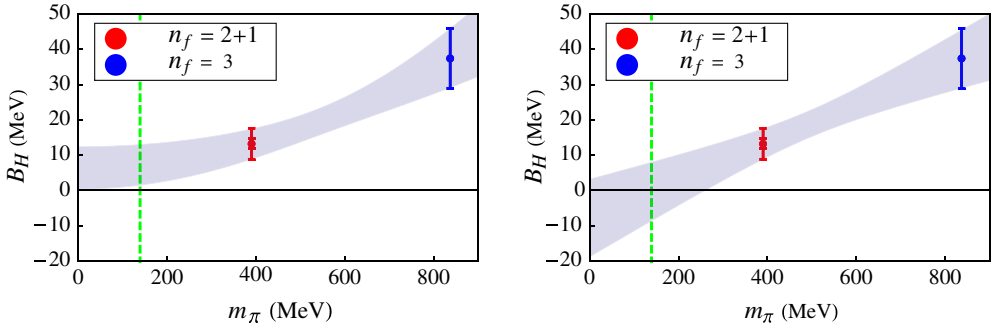

FIG. 13 (color online). Extrapolations of the LQCD results for the binding of the H-dibaryon. The left panel corresponds to an extrapolation that is quadratic in m_π, of the form $B_H(m_\pi) = B_0 + d_1 m_\pi^2$. The right panel is the same as the left panel except with an extrapolation of the form $B_H(m_\pi) = \tilde{B}_0 + \tilde{d}_1 m_\pi$. In each panel, the blue point and uncertainty result from the $n_f = 3$ LQCD calculation of Ref. [17], while the red point and uncertainty are our present $n_f = 2 + 1$ result. The green dashed vertical line corresponds to the physical pion mass.

shown in Fig. 13. Also shown in this figure are two naive extrapolations, one that is linear in m_π and one that is quadratic in m_π, as discussed in Ref. [19]. The extrapolations indicate that the LQCD calculations are presently not at sufficiently small quark masses to determine if the H-dibaryon is bound at the physical light-quark masses.

D. $\Xi^-\Xi^-$

Experimental information on the hyperon-hyperon interactions in the $s < -2$ sector does not exist, presenting a significant handicap to studies of the composition of neutron star matter. As an example of the importance of these interactions, Ref. [67] shows that when a strongly attractive $\Xi\Xi$ interaction is used in the Tolman-Oppenheimer-Volkoff equation, new stable solutions appear, corresponding to compact hyperon stars with masses similar to neutron stars but with smaller radii. From the theoretical point of view, the approximate flavor SU(3) symmetry of QCD indicates that a bound state in the $\Xi^-\Xi^-$ channel is likely. Phenomenological analyses of NN scattering and YN scattering provide a determination of the strength of the interaction for two baryons in the **27** irreducible representation of flavor SU(3) that also contains the $\Xi^-\Xi^-$ system. The OBE model developed by the Nijmegen group, NSC99 [2],[9] which includes explicit breaking of flavor SU(3) symmetry by using the physical meson and baryon masses, and chiral EFT [68], predicts a bound state in the $\Xi^-\Xi^-$ channel [3,4] at the physical pion mass.[10] However, only moderate attraction is obtained within a constituent quark model [69]. A small $\Xi^-\Xi^-$ interaction was calculated in the $20^3 \times 128$ ensemble [8] used in this work but may be subject to significant finite-volume uncertainties. LQCD calculations performed in the flavor SU(3) limit [70], in volumes of $16^3 \times 32$ with a lattice spacing of $b_s \sim 0.12$ fm and at pion masses of 1014 and 835 MeV, found attractive interactions in the flavor singlet t channel responsible for $\Xi^-\Xi^-$ interactions.

Our present LQCD calculations provide clear evidence for a bound $\Xi^-\Xi^-$ state at a pion mass of $m_\pi \sim 390$ MeV. The EMPs associated with the Ξ and the $\Xi^-\Xi^-$ system are shown in the left panels of Figs. 14 and 15.

The $\Xi^-\Xi^-$ binding energies extracted from the LQCD calculations are

$$\begin{aligned} B_{\Xi^-\Xi^-}^{(L=24)} &= 11.0 \pm 1.3 \pm 1.6 \text{ MeV}, \\ B_{\Xi^-\Xi^-}^{(L=32)} &= 13.0 \pm 0.5 \pm 3.9 \text{ MeV}. \end{aligned} \tag{23}$$

The volume extrapolation of the results in Eq. (23) is shown in Fig. 16, and it results in an extrapolated $\Xi^-\Xi^-$ binding energy of

$$B_{\Xi^-\Xi^-}^{(L=\infty)} = 14.0 \pm 1.4 \pm 6.7 \text{ MeV}, \tag{24}$$

where the first uncertainty is statistical and the second is systematic. This indicates that, at the $\sim 2\sigma$ level, the $\Xi^-\Xi^-$ channel supports a bound state. The fact that the binding energy calculated in the $24^3 \times 128$ ensemble has $k \cot\delta \gtrsim 0$ indicates that this volume is significantly modifying the $\Xi^-\Xi^-$ bound state and that calculations in larger volumes, or with nonzero total momentum, would refine the volume extrapolation. A positively shifted ground-state energy at the 2σ level was obtained from the $20^3 \times 128$ ensemble [8], which appears to be inconsistent with the results obtained from the $24^3 \times 128$ and $32^3 \times 256$ ensembles. We attribute this discrepancy to a combination of the $L \sim 2.5$ fm volume being too small to accommodate a $\Xi^-\Xi^-$ bound state, to the exponential corrections to Lüscher's energy-eigenvalue relation being large for this system, and to statistical fluctuations. The

[9]The recently developed extended soft-core models do not yet include the $s < -2$ sectors.

[10]The $\Xi\Xi(^3S_1)$ and NN $(^3S_1)$ states belong to different irreducible representations (10 and $\overline{\mathbf{10}}$, respectively), and therefore SU(3) flavor symmetry alone is unable to predict whether an analog of the deuteron in the $s = -4$ sector exists.

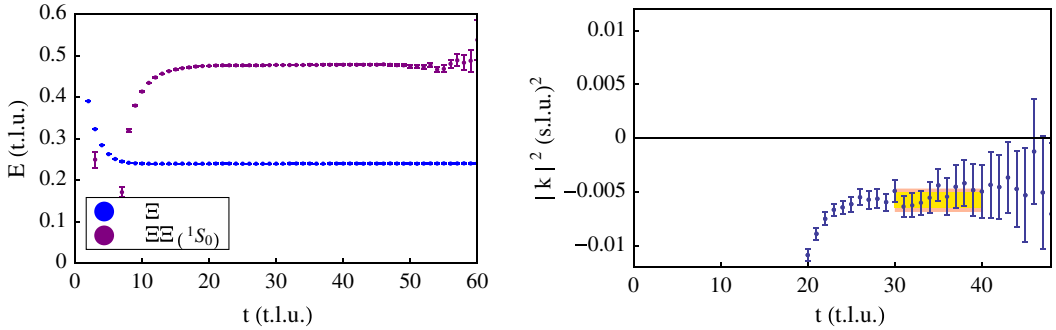

FIG. 14 (color online). The left panel shows an EMP of the Ξ and of the $\Xi^-\Xi^-$ system calculated with the $24^3 \times 128$ ensemble (in t.l.u.). The right panel shows the $|\mathbf{k}|^2$ [in (s.l.u.)^2] of the $\Xi^-\Xi^-$ system calculated with this ensemble, along with the fits.

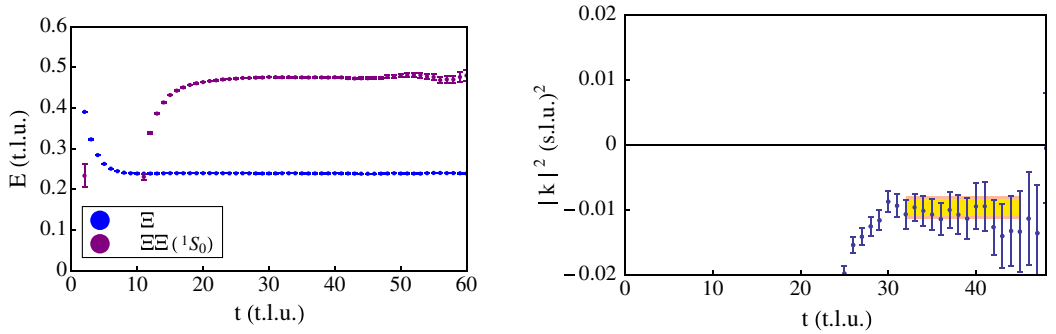

FIG. 15 (color online). The left panel shows an EMP of the Ξ and of the $\Xi^-\Xi^-$ system calculated with the $32^3 \times 256$ ensemble (in t.l.u.). The right panel shows the $|\mathbf{k}|^2$ [in (s.l.u.)^2] of the $\Xi^-\Xi^-$ system calculated with this ensemble, along with the fits.

later contribution could be explored with increased computational resources being devoted to the ensemble. One further possibility for the positively shifted ground-state energy in the $20^3 \times 128$ ensemble is that it was the lowest-lying continuum state and not the ground state of the system that had been identified. An important component of future work on these systems will be a systematic exploration and quantification of each of the possible issues.

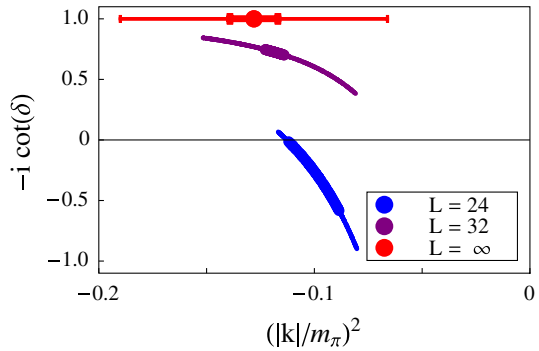

FIG. 16 (color online). The results of the lattice QCD calculations of $-i\cot\delta$ versus $|\mathbf{k}|^2/m_\pi^2$ in the $\Xi^-\Xi^-$ system obtained using Eq. (7), along with the infinite-volume extrapolation using Eq. (10). The inner uncertainty associated with each point is statistical, while the outer corresponds to the statistical and systematic uncertainties combined in quadrature.

This result and the predictions of OBE models and LO EFT are shown in Fig. 17. It is important to note that the uncertainty (and significance) of the LQCD result is comparable to that of the OBE models and EFT results. Further, this result demonstrates that LQCD is rapidly approaching the situation where it will provide more precise constraints on exotic systems than can be achieved in the laboratory. It will be interesting to see whether J-PARC [71] or FAIR [72] can provide constraints on the $s = -3$ and $s = -4$ systems, as well as on the possible H-dibaryon [73]. The binding energy in Eq. (24) provides strong motivation to return to OBE models and EFT frameworks and determine the expected dependence on the light-quark masses.

E. $\Sigma^-\Sigma^-$

As the $\Sigma^-\Sigma^-$ ($^1S_0$) system is in the **27** irreducible representation of flavor SU(3), it is also expected to be bound, but by somewhat less than the $\Xi^-\Xi^-$ system. While the NSC97a-NSC97f models [2] estimate the $\Sigma^-\Sigma^-$ binding, $B_{\Sigma^-\Sigma^-}$, to lie in the range 1.5 MeV $\lesssim B_{\Sigma^-\Sigma^-} \lesssim$ 3.2 MeV, large and negative scattering lengths are found in the $\Sigma^-\Sigma^-$ channel with LO EFT [74] in the absence of Coulomb interactions and isospin breaking

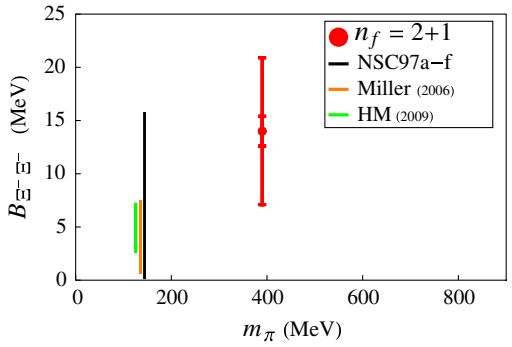

FIG. 17 (color online). The $\Xi^-\Xi^-$ binding energy as a function of the pion mass. The black line denotes the predictions of the NSC97a-NSC97f models [2] constrained from nucleon-nucleon and hyperon-nucleon scattering data. The orange line denotes the range of predictions by Miller [3], and the green line denotes the leading order EFT prediction by Haidenbauer and Meißner (HM) [4]. The red point and uncertainty (the inner is statistical and the outer is statistical and systematic combined in quadrature) are our present $n_f = 2 + 1$ result. The OBE model and EFT predictions at the physical pion mass are displaced horizontally for the purpose of display.

(these results exhibit non-negligible dependence on the momentum cutoff). On the other hand, the constituent quark model of Ref. [69] finds strong similarities between the behavior of the $\Sigma^-\Sigma^-$ and nn interactions, leading to similar values for the phase shifts. Our LQCD calculations in this channel are inconclusive. While the ground state in the $24^3 \times 128$ ensemble is negatively shifted at the 1σ level, the ground state in the $32^3 \times 256$ ensemble is consistent with zero, and thus is consistent with both a scattering state and a bound state. However, the large and positive energy shift obtained from the $20^3 \times 128$ ensemble [8] suggests that the $\Sigma^-\Sigma^-$ state we have identified is a scattering state and not a bound state, assuming that the exponential volume modifications to Lüscher's energy-eigenvalue relation are small.

V. CONCLUSIONS

We have performed precise lattice QCD calculations of baryon-baryon systems at a pion mass of $m_\pi \sim 390$ MeV in four ensembles of anisotropic clover gauge-field configurations with a spatial lattice spacing of $b_s \sim 0.123$ fm, an anisotropy of $\xi \sim 3.5$, and cubic spatial lattice volumes with extent $L \sim 2.0$, 2.5, 2.9, and 3.9 fm. These calculations have provided evidence, with varying levels of significance, for the existence of two-baryon bound states from QCD, which are summarized in Table III. Our LQCD calculations were performed at one lattice spacing, $b_s \sim 0.123$ fm, but discretization effects are expected to be small as they scale as $\mathcal{O}(b_s^2)$ for the clover action. Consequently, we do not expect them to significantly alter our conclusions. A second lattice spacing is required to quantify this systematic uncertainty.

By far the most significant result is that the H-dibaryon is bound at the 3σ level at this pion mass, improving on results we have already presented in Ref. [16]. At the $\sim 2\sigma$ level of significance, we find that the $\Xi^-\Xi^-$ system is also bound, which is qualitatively consistent with an array of hadronic models and EFT analyses of this system at the physical light-quark masses. It is interesting to note that the level of precision of the $\Xi^-\Xi^-$ binding from LQCD is comparable to the level of precision associated with the phenomenological predictions. With increasing computational resources directed at these two-baryon systems, the QCD prediction will become more precise and eventually become input for phenomenological models and be used to constrain the coefficients appearing in the effective field theories.

A major goal of lattice QCD is to postdict the anomalously small binding energy of the deuteron. We have presented $\sim 1\sigma$ level evidence for a bound deuteron from QCD, which is well below "discovery level," and our result should be considered a first step toward a definitive calculation. Nevertheless, it is now unambiguously clear that a precise determination of the deuteron binding energy can be performed with sufficient computational resources. Our result hints that the deuteron is bound, as does the result of a previous quenched calculation, at heavy pion masses, in contrast with phenomenological analyses and with EFT predictions. We also find suggestions of bound dineutrons which are far from definitive, but are consistent with the quenched result at a heavier pion mass [12]. If this remains the case when the calculation is refined, there are light-quark masses between $m_\pi \sim 140$ MeV and $m_\pi \sim 390$ MeV for which the scattering length in this channel would be infinite and the system would be scale invariant at low energies.

Phenomenology based upon flavor SU(3) symmetry indicates that the $\Xi^-\Xi^-$ system should be more bound than the $\Sigma^-\Sigma^-$ system, which in turn should be more bound than the dineutron (which is nearly bound) at the physical light-quark masses, as these three systems are all members of the same 27 irreducible representation of SU(3). Our results are consistent with this within the uncertainties of the LQCD calculations, but further work is required before definitive conclusions can be drawn.

TABLE III. A summary of the two-body binding energies determined in this work.

	Deuteron	Dineutron	H-dibaryon	$\Xi^-\Xi^-$
Binding energy (MeV)	11(05)(12)	7.1(5.2)(7.3)	13.2(1.8)(4.0)	14.0(1.4)(6.7)

The results of the lattice QCD calculations presented in this paper, which refine and broaden our previous work [16], provide clear evidence for bound states of two baryons directly from QCD. With the suggestion of a deuteron and a bound dineutron at this heavier pion mass, there is compelling motivation to invest larger computational resources into pursuing lattice QCD calculations at light-quark masses, and to perform such calculations in multiple volumes and with multiple lattice spacings. It is clear that enhanced computational resources will enable calculations of the properties and interactions of nuclei from QCD with quantifiable and systematically removable uncertainties.

ACKNOWLEDGMENTS

We would like to thank G. A. Miller for interesting discussions. We thank K. Roche for computing resources at ORNL NCCS, and B. Joó for a significant contribution to our running. We thank R. Edwards and B. Joó for help with QDP + + and Chroma [75]. We acknowledge computational support from the USQCD SciDAC project, the National Energy Research Scientific Computing Center (NERSC, Office of Science of the US DOE, DE-AC02-05CH11231), the UW HYAK facility, Centro Nacional de Supercomputación (Barcelona, Spain), LLNL, the NSF through Teragrid resources provided by TACC and NICS under Grant No. TG-MCA06N025, and the Argonne Leadership Computing Facility at Argonne National Laboratory (Office of Science of the U. S. DOE, DE-AC02-06CH11357). S. R. B. was supported in part by the NSF CAREER Grant No. PHY-0645570. The work of E. C. and A. P. is supported by Contract No. FIS2008-01661 from MEC (Spain) and FEDER. A. P. acknowledges support from the RTN Flavianet MRTN-CT-2006-035482 (EU). H-W. L. and M. J. S. were supported in part by the DOE Grant No. DE-FG03-97ER4014. W. D. and K. O. were supported in part by DOE Grants No. DE-AC05-06OR23177 (JSA) and No. DE-FG02-04ER41302. W. D. was also supported by DOE OJI Grant No. DE-SC0001784 and Jeffress Memorial Trust, Grant No. J-968. K. O. was also supported in part by NSF Grant No. CCF-0728915 and DOE OJI Grant No. DE-FG02-07ER41527. A. T. was supported by NSF Grant No. PHY-0555234 and DOE Grant No. DE-FC02-06ER41443. The work of T. L. was performed under the auspices of the U. S. Department of Energy by LLNL under Contract No. DE-AC52-07NA27344. The work of A. W. L. was supported in part by the Director, Office of Energy Research, Office of High Energy and Nuclear Physics, Divisions of Nuclear Physics, of the U. S. DOE under Contract No. DE-AC02-05CH11231.

[1] R. L. Jaffe, Phys. Rev. Lett. **38**, 195 (1977); **38**, 617(E) (1977).
[2] V. G. J. Stoks and T. A. Rijken, Phys. Rev. C **59**, 3009 (1999).
[3] G. A. Miller, arXiv:nucl-th/0607006.
[4] J. Haidenbauer and U.-G. Meißner, Phys. Lett. B **684**, 275 (2010).
[5] M. Fukugita, Y. Kuramashi, H. Mino, M. Okawa, and A. Ukawa, Phys. Rev. Lett. **73**, 2176 (1994).
[6] M. Fukugita, Y. Kuramashi, M. Okawa, H. Mino, and A. Ukawa, Phys. Rev. D **52**, 3003 (1995).
[7] S. R. Beane, P. F. Bedaque, K. Orginos, and M. J. Savage, Phys. Rev. Lett. **97**, 012001 (2006).
[8] S. R. Beane *et al.* (NPLQCD Collaboration), Phys. Rev. D **81**, 054505 (2010).
[9] S. Aoki, T. Hatsuda, and N. Ishii, Comp. Sci. Disc. **1**, 015009 (2008).
[10] S. Aoki, T. Hatsuda, and N. Ishii, Prog. Theor. Phys. **123**, 89 (2010).
[11] N. Ishii, S. Aoki, and T. Hatsuda, Phys. Rev. Lett. **99**, 022001 (2007).
[12] T. Yamazaki, Y. Kuramashi, and A. Ukawa, Phys. Rev. D **84**, 054506 (2011).
[13] T. Yamazaki, Y. Kuramashi, and A. Ukawa, Phys. Rev. D **81**, 111504 (2010).
[14] S. R. Beane *et al.*, Phys. Rev. D **80**, 074501 (2009).
[15] P. de Forcrand and M. Fromm, Phys. Rev. Lett. **104**, 112005 (2010).
[16] S. R. Beane *et al.* (NPLQCD Collaboration), Phys. Rev. Lett. **106**, 162001 (2011).
[17] T. Inoue *et al.* (HAL QCD Collaboration), Phys. Rev. Lett. **106**, 162002 (2011).
[18] T. Inoue (HAL QCD Collaboration), arXiv:1109.1620.
[19] S. R. Beane *et al.*, Mod. Phys. Lett. A **26**, 2587 (2011).
[20] P. E. Shanahan, A. W. Thomas, and R. D. Young, Phys. Rev. Lett. **107**, 092004 (2011).
[21] S. R. Beane *et al.*, Phys. Rev. D **79**, 114502 (2009).
[22] S. R. Beane *et al.*, Phys. Rev. D **84**, 014507 (2011).
[23] H. W. Hamber, E. Marinari, G. Parisi, and C. Rebbi, Nucl. Phys. **B225**, 475 (1983).
[24] M. Lüscher, Commun. Math. Phys. **105**, 153 (1986).
[25] M. Lüscher, Nucl. Phys. **B354**, 531 (1991).
[26] M. Lüscher, Commun. Math. Phys. **104**, 177 (1986).
[27] S. R. Beane, P. F. Bedaque, A. Parreno, and M. J. Savage, Phys. Lett. B **585**, 106 (2004).
[28] S. Bour, S. Konig, D. Lee, H. W. Hammer, and U. G. Meißner, Phys. Rev. D **84**, 091503(R) (2011).
[29] Z. Davoudi and M. J. Savage, Phys. Rev. D **84**, 114502 (2011).
[30] M. Okamoto *et al.* (CP-PACS Collaboration), Phys. Rev. D **65**, 094508 (2002).
[31] P. Chen, Phys. Rev. D **64**, 034509 (2001).

[32] C. Morningstar and M. J. Peardon, Phys. Rev. D **69**, 054501 (2004).
[33] H. W. Lin *et al.* (Hadron Spectrum Collaboration), Phys. Rev. D **79**, 034502 (2009).
[34] R. G. Edwards, B. Joó, and H. W. Lin, Phys. Rev. D **78**, 054501 (2008).
[35] J. J. Dudek, R. G. Edwards, M. J. Peardon, D. G. Richards, and C. E. Thomas, Phys. Rev. Lett. **103**, 262001 (2009).
[36] J. Bulava *et al.*, Phys. Rev. D **82**, 014507 (2010).
[37] J. J. Dudek, R. G. Edwards, B. Joo, M. J. Peardon, D. G. Richards, and C. E. Thomas, Phys. Rev. D **83**, 111502 (2011).
[38] C. Morningstar, J. Bulava, J. Foley, K. J. Juge, D. Lenkner, M. Peardon, and C. H. Wong, Phys. Rev. D **83**, 114505 (2011).
[39] R. G. Edwards, J. J. Dudek, D. G. Richards, and S. J. Wallace, Phys. Rev. D **84**, 074508 (2011).
[40] H.-W. Lin and S. D. Cohen, arXiv:1108.2528.
[41] S. R. Beane, W. Detmold, K. Orginos, and M. J. Savage, Prog. Part. Nucl. Phys. **66**, 1 (2011).
[42] P. F. Bedaque, I. Sato, and A. Walker-Loud, Phys. Rev. D **73**, 074501 (2006).
[43] I. Sato and P. F. Bedaque, Phys. Rev. D **76**, 034502 (2007).
[44] C. Aubin and K. Orginos, AIP Conf. Proc. **1374**, 621 (2011).
[45] K. Orginos, Proc. Sci., LATTICE2010 (2010) 118.
[46] S. R. Beane and M. J. Savage, Nucl. Phys. **A713**, 148 (2003).
[47] E. Epelbaum, U. G. Meißner, and W. Gloeckle, Nucl. Phys. **A714**, 535 (2003).
[48] S. R. Beane and M. J. Savage, Nucl. Phys. **A717**, 91 (2003).
[49] J. W. Chen, T. K. Lee, C. P. Liu, and Y. S. Liu, arXiv:1012.0453.
[50] V. V. Flambaum and R. B. Wiringa, Phys. Rev. C **76**, 054002 (2007).
[51] P. F. Bedaque, T. Luu, and L. Platter, Phys. Rev. C **83**, 045803 (2011).
[52] M. K. Cheoun, T. Kajino, M. Kusakabe, and G. J. Mathews, Phys. Rev. D **84**, 043001 (2011).
[53] E. Braaten and H. W. Hammer, Phys. Rev. Lett. **91**, 102002 (2003).
[54] S. Bashinsky and R. L. Jaffe, Nucl. Phys. **A625**, 167 (1997).
[55] K. Yamamoto *et al.*, Phys. Lett. B **478**, 401 (2000).
[56] T. Sakai, K. Shimizu, and K. Yazaki, Prog. Theor. Phys. Suppl. **137**, 121 (2000).
[57] P. J. Mulders and A. W. Thomas, J. Phys. G **9**, 1159 (1983).
[58] A. L. Trattner, Ph.D. thesis, LBL, 2006, Report No. UMI-32-54109.
[59] C. J. Yoon *et al.*, Phys. Rev. C **75**, 022201 (2007).
[60] P. B. Mackenzie and H. B. Thacker, Phys. Rev. Lett. **55**, 2539 (1985).
[61] Y. Iwasaki, T. Yoshie, and Y. Tsuboi, Phys. Rev. Lett. **60**, 1371 (1988).
[62] A. Pochinsky, J. W. Negele, and B. Scarlet, Nucl. Phys. B, Proc. Suppl. **73**, 255 (1999).
[63] I. Wetzorke, F. Karsch, and E. Laermann, Nucl. Phys. B, Proc. Suppl. **83**, 218 (2000).
[64] I. Wetzorke and F. Karsch, Nucl. Phys. B, Proc. Suppl. **119**, 278 (2003).
[65] Z. H. Luo, M. Loan, and X. Q. Luo, Mod. Phys. Lett. A **22**, 591 (2007).
[66] J. Mondejar and J. Soto, Eur. Phys. J. A **32**, 77 (2007).
[67] J. Schaffner-Bielich, M. Hanauske, H. Stoecker, and W. Greiner, Phys. Rev. Lett. **89**, 171101 (2002).
[68] M. J. Savage and M. B. Wise, Phys. Rev. D **53**, 349 (1996).
[69] Y. Fujiwara, Y. Suzuki, and C. Nakamoto, Prog. Part. Nucl. Phys. **58**, 439 (2007).
[70] T. Inoue *et al.* (HAL QCD Collaboration), Prog. Theor. Phys. **124**, 591 (2010).
[71] http://j-parc.jp/NuclPart/index_e.html.
[72] J. Steinheimer, M. Mitrovski, T. Schuster, H. Petersen, M. Bleicher, and H. Stoecker, Phys. Lett. B **676**, 126 (2009).
[73] http://j-parc.jp/NuclPart/pac_1107/pdf/KEK_J-PARC-PAC2011-03.pdf.
[74] H. Polinder, J. Haidenbauer, and U. G. Meißner, Phys. Lett. B **653**, 29 (2007).
[75] R. G. Edwards and B. Joó, Nucl. Phys. B, Proc. Suppl. **140**, 832 (2005).